JOURNAL OF MATERIALS SCIENCE 32 (1997) 6645–6651

Age-hardening characteristics of aluminium–chromium alloys

M. K. BANERJEE
Metallurgy Department, B.E. College (Deemed University)
P.O. Botanic Garden, Howrah-711 103, India

The age-hardening behaviour of Al–Cr alloys containing varying amounts of chromium has been studied, and the effect of silicon on the ageing response of the alloy system was also investigated. Hardness measurement and tensile properties evaluation were used to describe the ageing response of the alloys. With the aid of microstructural observation, the ageing mechanism has been explained. Results of isothermal ageing were used to describe the kinetics of precipitation in both the binary and ternary alloys. It was noticed that the age hardening in aluminium–chromium alloys was mainly due to the precipitation of intermetallics on to the dislocations. The ageing response of the binary alloy containing chromium in excess of its solubility limit was rather poor. However, addition of silicon helped to improve the ageing response of the alloys. Silicon was found to stimulate nucleation of ageing precipitates in the investigated alloys.

1. Introduction

In view of the presence of a sloping solvus in the phase diagram, there had been considerable interest in the study of the age-hardening behaviour in aluminium–chromium alloy which possesses excellent corrosion and oxidation resistance [1]. The age-hardening behaviour of Al–0.5 Cr was studied earlier through hardness, electrical resistivity and transmission electron microscopy [2]. It was reported that precipitation took place at lattice defects and were of two morphologies, depending on the ageing temperature. Cold working was also found to accelerate the age-hardening behaviour. It was demonstrated earlier that the alloys which showed improvement in ageing response upon cold working were responsive to minor additions of other elements during their ageing [3]. It is also known that the inherent proneness to the formation of the intermetallic $CrAl_7$ in binary Al–Cr alloy deteriorates the ageing response of the alloy at high temperature [4]. Silicon is reported to have a significant role on the age-hardening behaviour of this alloy.

However, the ageing behaviour of the binary alloys with varying chromium contents has not been studied systematically. Also, the effect of varying silicon content and its exact role on the phase decomposition in Al–Cr alloys has not been explored. The structure–mechanical property correlation is not well documented in the available literature. Therefore, it appears worthwhile to investigate the exact mechanism of age hardening in binary Al–Cr alloys of varying chromium content. The effect of silicon on the precipitation behaviour in Al–Cr alloys also needs to be quantitatively assessed. With these views in mind, the present work was performed to characterize age-hardenable Al–Cr alloys at varying chromium and silicon levels.

2. Experimental procedure

Aluminium chromium alloys were prepared in a resistance heating electric furnace by melting electrolytically pure aluminium under a suitable flux cover. A requisite quantity of chemically pure chromium powder was compacted with aluminium. These compacts were added to the molten aluminium bath. After complete melt down, the alloy was stirred and degassed. The alloy was then solidified and remelted to produce a uniform chemical composition. The remelted alloy was poured in preheated 25 mm square moulds of cast iron. A few melts were produced with varying silicon content by mixing silicon powder with those of chromium and then preparing the melts in a similar manner. In one melt, zirconium was added by following the same technique. The chemical composition of the alloys is given in Table I.

The cast alloys were hot rolled at 350 °C to reduce the thickness of the strips to 6 mm. The rolled alloys were cut into suitable pieces, solution treated at 610 °C for 5 h, and then quenched in iced brine. The hardness of each of the quenched alloys was recorded during natural ageing at room temperature. The alloys were aged isochronally for 2 h within the temperature interval 200–500 °C. In addition, the alloys were isothermally aged at various temperatures in the range 375–475 °C. The hardness value of the aged alloys were measured on a Rockwell "F" scale. An average of ten consistent hardness values was used as the representative hardness of the aged alloys. Tensile tests were carried out with the isochronally aged alloys in an Instron testing machine at a strain rate of $0.6 \times 10^{-3}\,s^{-1}$. Transmission electron microscopy was done in a Jeol 200 microscope by thinning with a jet of HNO_3 and CH_3OH (30 : 70) at -10 °C.

0022–2461

TABLE I Chemical composition (wt %) of the alloys

Alloy	Cu	Fe	Mg	Mn	Ni	Si	Ti	Zn	Cr	Zr	Remarks
1.	0.001	0.21	0.03	0.006	0.001	0.08	0.008	0.002	0.63	0.003	Al–Cr
2.	0.003	0.19	0.003	0.004	0.002	0.13	0.004	0.120	0.78	0.001	Al–Cr
3.	0.001	0.25	0.004	0.005	0.001	0.09	0.019	0.001	0.90	0.004	Al–Cr
4.	0.001	0.21	0.003	0.004	0.001	0.20	0.007	0.003	0.77	0.003	Al–Cr
5.	0.002	0.18	0.008	0.003	0.002	0.19	0.009	0.003	0.90	0.001	Al–Cr
6.	0.024	0.24	0.006	0.005	0.001	0.56	0.007	0.019	0.90	0.003	Al–Cr–Si
7.	0.002	0.19	0.006	0.003	0.001	0.76	0.007	0.003	1.20	0.001	Al–Cr–Si
8.	0.003	0.19	0.006	0.003	0.001	0.76	0.007	0.016	0.90	0.001	Al–Cr–Si
9.	0.001	0.20	0.007	0.004	0.001	0.60	0.008	0.003	0.78	0.003	Al–Cr–Si
10.	0.001	0.18	0.004	0.004	0.001	0.82	0.008	0.003	0.78	0.003	Al–Cr–Si
11.	0.019	0.22	0.005	0.004	0.004	0.26	0.004	0.043	0.80	0.34	Al–Cr–Si–Zr

Microhardness testing was also carried out in some aged samples using a Micro duramet 400 attached to the Polyver met microscope utilizing a knoop indentor.

3. Results

3.1. Isothermal ageing

The effect of natural ageing at room temperature for the alloys under investigation is shown in Fig. 1. It is noted that hardness variation due to natural ageing is particularly insignificant in the present series of alloys. This implies that unlike a number of common aluminium-based age-hardenable alloys, the investigated aluminium–chromium alloys do not form Guinier–Preston zones (G–P) at room temperature.

The time dependence of age hardening at a temperature of 375 °C is shown for various alloys in Figs 2–4. It is observed that in binary alloys 1 and 2, when the silicon content is rather low, the ageing response is higher for alloy 2 containing higher chromium. However, for alloy 3 which contains excess solute beyond the primary solubility limit, it can be noticed that the onset of precipitation hardening is delayed until 50 min ageing, beyond which the hardness value starts rising. When a small amount of silicon ($\sim 0.2\%$) is added to alloys 2 and 3 it is observed that alloy 4 exhibits a higher level of age hardening with increased ageing rate than alloy 5 which shows an incubation period up to about 50 min ageing. However, comparison of the ageing curves of alloys 5 and 3 reveals that the ageing response is more pronounced in alloy 5, which contains higher silicon, at the same chromium level. At the same chromium level of alloy 5 when the silicon content is increased to 0.56% as in alloy 6, the age-hardening response is smaller but the hardness levels are higher at all ageing times with no

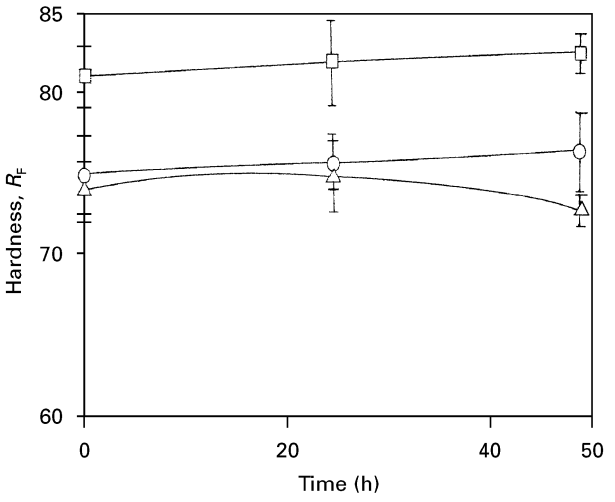

Figure 1 Hardness–time curves of the alloys aged at room temperature. (△) Alloy 3, (○) alloy 6, (□) alloy 8.

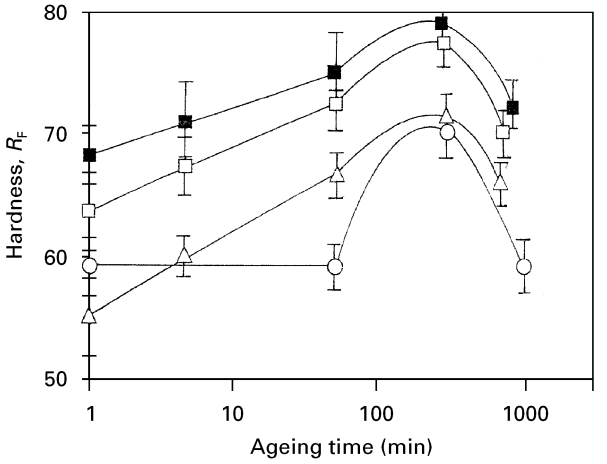

Figure 2 Hardness–time curves of the alloys aged at 375 °C. (△) Alloy 1, (□) alloy 2, (○) alloy 3, (■) alloy 9.

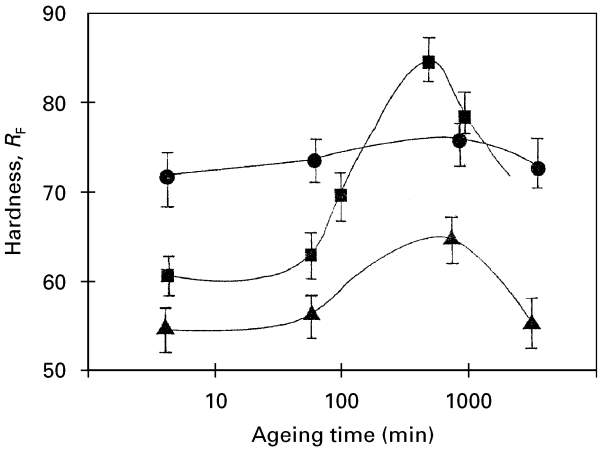

Figure 3 Hardness–time curves of the alloys aged at 375 °C. (▲) Alloy 5, (■) alloy 4, (●) alloy 6.

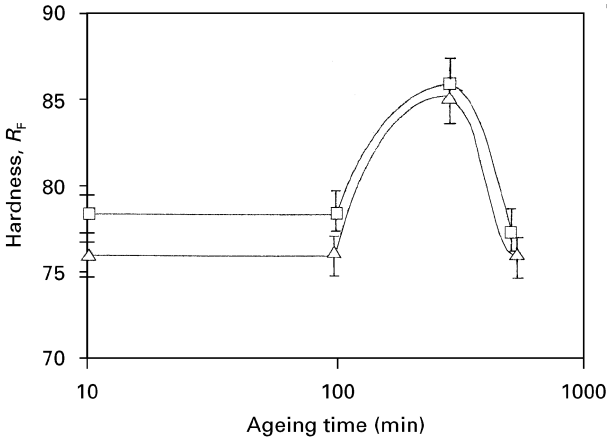

Figure 4 Hardness–time curves of the alloys aged at 375 °C. (△) Alloy 7, (□) alloy 8.

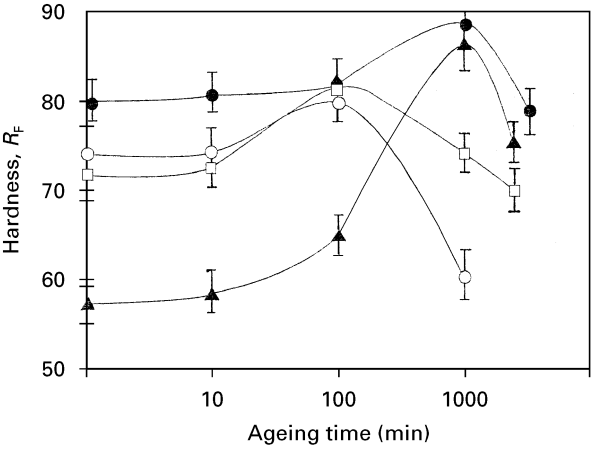

Figure 5 Hardness–time curves of the alloys aged at 470 °C. (○) Alloy 3, (▲) alloy 4, (●) alloy 5, (□) alloy 6.

incubation period. When chromium is below the primary solubility limit (alloy 2), the addition of 0.60 wt% silicon (similar to alloy 6) induces rather good age hardening in alloy 9 (Fig. 2). At still higher silicon levels (~ 0.76%), a rather poor age-hardening response is observed for alloys 7 and 8 (Fig. 4). Following an incubation period of 120 min, the hardness starts rising but to a smaller extent. The fall in hardness beyond the peaks at 210 min has also been found to be rather small and slow.

When the alloys are aged at higher temperature, interesting observations can be made (Figs 5 and 6). For alloy 3, containing a high amount of insoluble intermetallics, the ageing response is very poor. Although the hardness level is higher than that in the alloy correspondingly aged at 375 °C, the hardness increase due to ageing is rather small. Although a similar trend is noticed for alloy 5 at 0.2% silicon level, the age hardening is slightly better. Interestingly, if the silicon level is increased to 0.56%, the age-hardening response is found to have increased more without any incubation period similar to that observed when the same alloy 6 was aged at 375 °C. The situation becomes still clearer in alloys containing 0.78% wt% chromium where increasing silicon content has led to increasing age-hardening effect, when aged at 470 °C (Fig. 6).

It appears, therefore, that silicon reduces the quench sensitivity of the Al–Cr alloy. It also increases the hardening response in alloy 2. A slight increase in silicon from the level of alloy 2 considerably increases the level of hardening (alloy 4). However, it possesses a slightly lower hardness value than the corresponding alloy 5 containing the same amount of silicon. In alloy 1 containing no silicon and low chromium, prominent ageing is observed at a remarkably accelerated rate. The ageing rate is maximum in this alloy and, even compared to alloy 2 containing a similar silicon content, it is observed that this alloy containing a lower amount of chromium exhibits a greater ease of precipitation, even at an earlier ageing time.

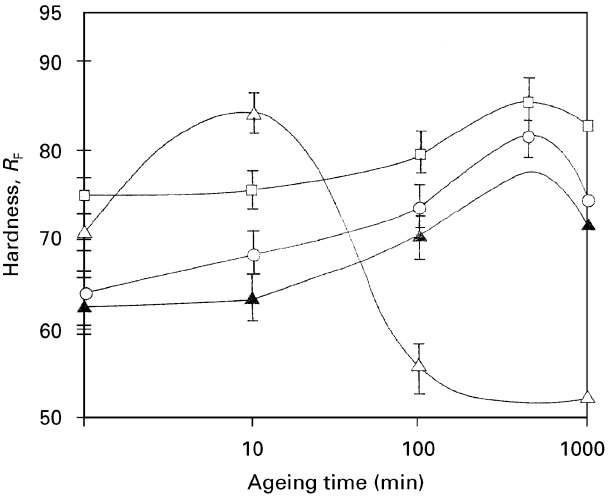

Figure 6 Hardness–time curves of the alloys aged at 470 °C. (△) Alloy 1, (▲) alloy 2, (○) alloy 9, (□) alloy 10.

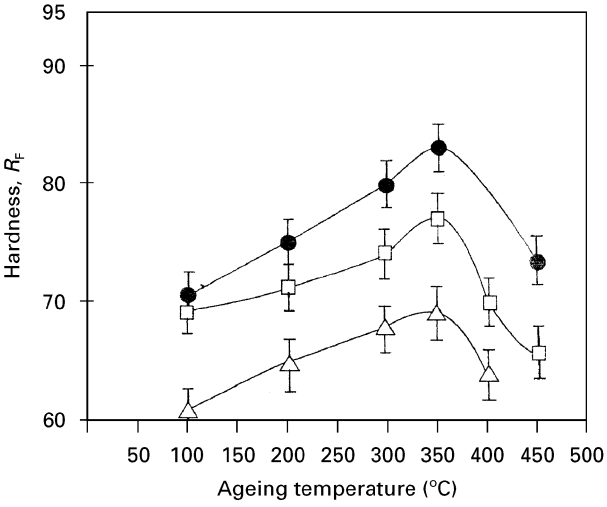

Figure 7 Hardness–temperature curves for 1 h isochronal ageing. (△) Alloy 1, (●) alloy 2, (□) alloy 3.

3.2. Isochronal ageing

The result of isochronal ageing is shown in Fig. 7. It is noticed that with increasing chromium content, the extent of maximum hardening increases (compare alloy 1 and 2) until the chromium content is such as to leave a considerable amount of insoluble intermetallics (alloy 3), after which the age-hardening

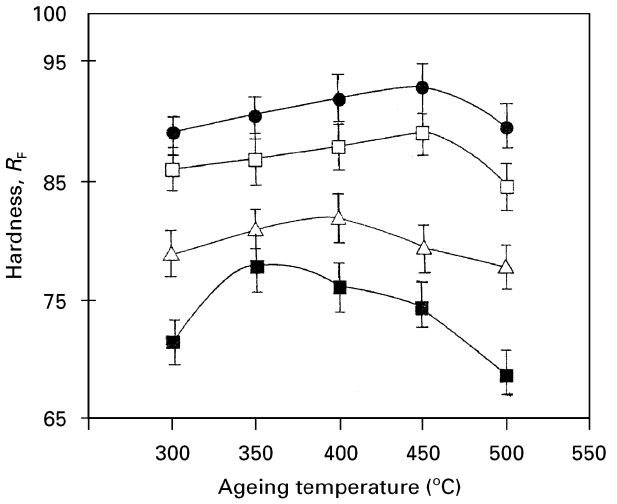

Figure 8 Hardness–temperature curves for 1 h isochronal ageing. (■) Alloy 3, (△) alloy 5, (□) alloy 6, (●) alloy 11.

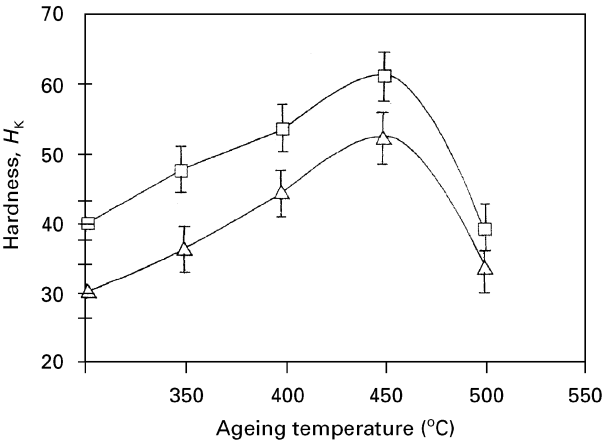

Figure 9 Microhardness–temperature curves for alloys isochronally aged for 1 h. (□) Alloy 2, (△) alloy 3.

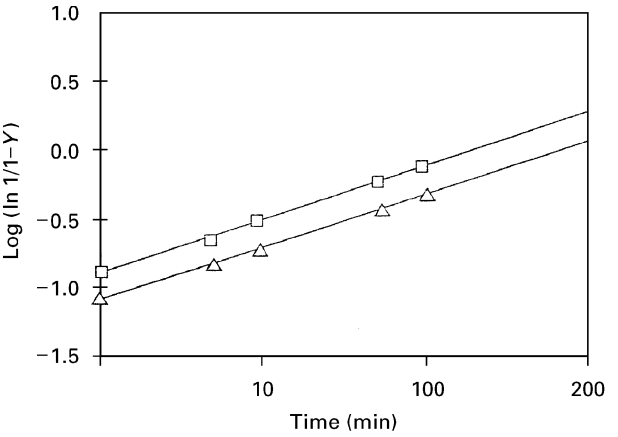

Figure 10 Logarithmic plot of rate data. (□) Alloy 2, (△) alloy 9.

response becomes inferior. In binary alloys, the increasing chromium content does not seem to have altered the peak hardness temperature. However, the effect of increasing silicon is observed to have shifted the peak hardness temperature to high values, although at the same chromium level, the overall hardness value at all ageing temperatures is higher for higher silicon alloys (Fig. 8). The addition of zirconium to alloy 6 seems to have given rise to higher hardening and the peak hardness temperature remains essentially the same.

Fig. 9 demonstrates the ageing behaviour of binary alloys where the ageing curves are drawn from the results of microhardness tests carried out on the matrix. Care was taken to keep the indentation away from coarse particles. Alloy 3, which did not show much ageing response under macrohardeness testing, shows an appreciable ageing response in microhardness testing of the matrix solid solution. The curves imply age hardening due to solute rejection in a matrix otherwise free from interference from coarse insolubles.

3.3. Precipitation kinetics

From observation of the ageing curves it appears that the extent of excess solutes rejected during isochronal ageing can be correlated with the extent of hardness increase in the alloys. Based on the maximum achievable hardness over the hardness of the alloys in the quenched state, the fraction of excess solute precipitated during isothermal ageing was determined. The rate of the precipitation reaction is described by an Avramis' equation. The fraction transformed at time t, is given by $Y = \text{Aexp}\ (kt^n)$, where k and n are the characteristic nucleation and growth parameters of the precipitation reaction. The curves in Fig. 10 are based on the data of excess solute rejected at various times of ageing at a particular temperature. From these curves, it is observed that the value of n for binary alloy 2 is 0.526, and is 0.535 for alloy 9 containing higher silicon. This identical growth parameter in either alloy is indicative of the fact that the growth behaviour of the aluminium chromium alloy is not altered by silicon addition. On the contrary there is about a 20% increase in the nucleation parameter k in the silicon-doped alloy. This indicates that silicon stimulates the nucleation of precipitates in the above alloy.

Similar isothermal ageing carried out at different temperatures between 375 and 475 °C has enabled the calculation of sets of n and k values at different temperatures. Plotting ln (rate) against $10^3/T$ gave the Arrhenius curve as shown in Fig. 11. It is observed that the activation energy for either alloy is nearly the same, 70–72 kJ mol^{-1}, inspite of the appreciable difference in their silicon contents.

Fig. 12 shows the variation of ultimate tensile strength and total elongation against ageing temperature. In general, it is observed that maximum tensile strengths are accompanied by correspondingly higher values of elongation. This is indicative of an Orowan by-passing mechanism being operative in the alloys under investigation. The variation of yield stress is also shown in Fig. 13. From this figure it is noticed that alloys containing insoluble intermetallics show an incubation period, whereas others do not show such trend. Alloy 1 containing no silicon is found to possess a higher yield strength although the solute per cent is higher in alloy 4. However, alloy 4 shows a constancy

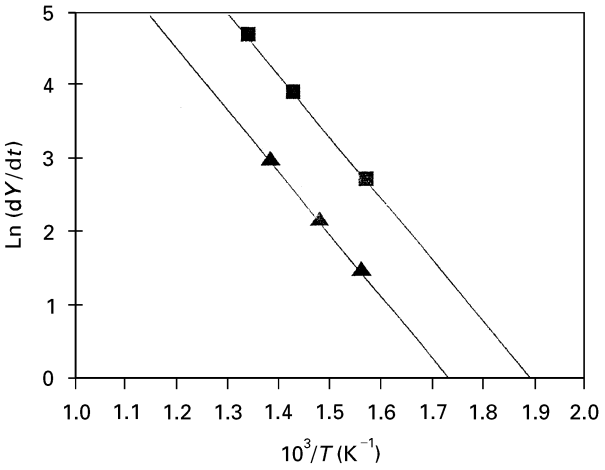

Figure 11 Arrhenius plots of rate data. (■) Alloy 2, (▲) alloy 9.

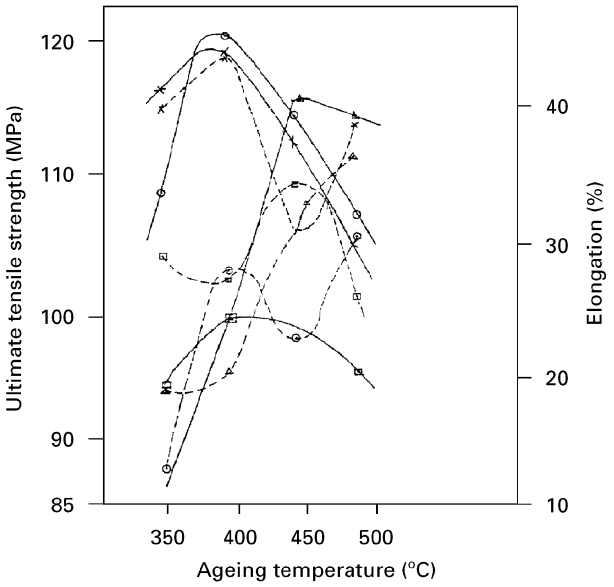

Figure 12 Tensile properties of Al–Cr alloys against ageing temperature. (○) Alloy 4, (□) alloy 7, (△) alloy 8, (×) alloy 11. (——) Tensile strength, (– – –) elongation.

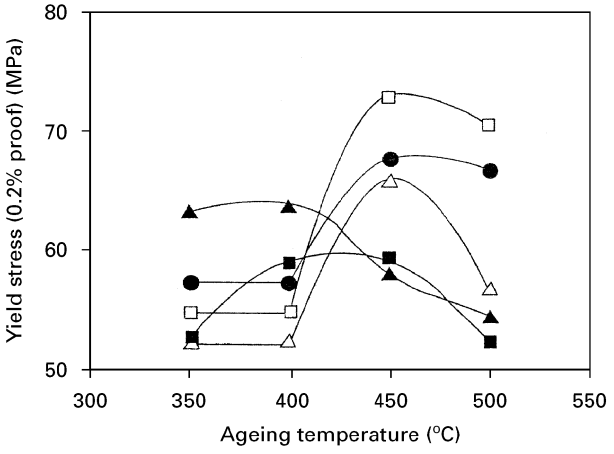

Figure 13 Variation of yield stress (0.2% proof) with ageing temperature. (▲) Alloy 1, (■) alloy 4, (□) alloy 5, (●) alloy 7, (△) alloy 9.

in yield stress at a higher temperature regime (440–450 °C) against 350–400 °C for alloy 1.

The variation of strain-hardening exponent n was obtained from $\sigma = k\varepsilon^n$ and it was observed that, in general, the values of n decrease in the temperature region where the corresponding yield stresses of the alloys increase. However, in alloy 1, it is observed that n increases, while the yield stress also increases (Fig. 14).

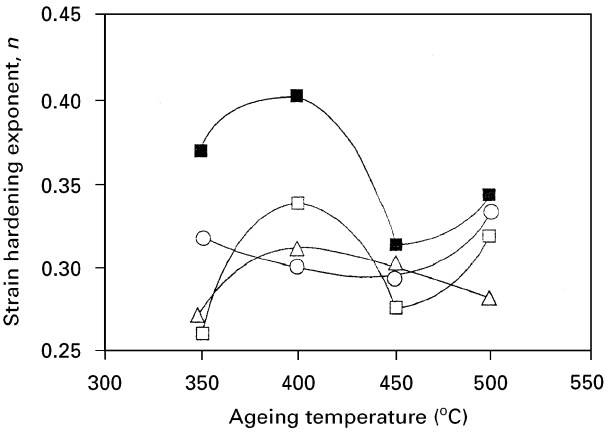

Figure 14 Strain-hardening exponent at room temperature plotted against the temperature of isochronal ageing for 1 h. (□) Alloy 4, (○) alloy 5, (■) alloy 7, (△) alloy 9.

4. Discussion

Reportedly, the binding energy between the chromium atoms and the quenched-in vacancies is high. In addition, the higher tendency for the formation of $CrAl_7$ in the Al–Cr alloys aids in the annhilation of quenched-in vacancies at the intermetallic/matrix interface. As a result, G–P zone formation is not possible. In the present alloy series, we have not noticed the formation of G–P zones, but there is definite evidence of age hardening. Therefore, it appears that the age hardening in the present alloys is due to the precipitation, in fairly fine dispersion, on the dislocation loops and on dislocation substructure as observed elsewhere [5]. This is shown in Fig. 15, where the quenched alloy exhibits dislocation substructure with less populated Frank loops. It therefore appears that in Al–Cr alloy, age hardening is predominantly due to the precipitation, in fine form, of the intermetallics on the dislocations. The increased dislocation density near the coarse precipitates also contributes to the higher degree of precipitation.

While ageing, the increased volume fraction of precipitates leads to increased hardening and the fall in hardness beyond the peak is mainly due to particle coarsening.

It is observed that the age-hardening response at 375 °C of alloys containing excess solute is improved by adding silicon. The ageing at high temperature verifies that poor age-hardening response is due to a high alloy content where already existing intermetallics are present. These intermetallics assist in the premature precipitation of solutes on to them during quenching and mainly while subsequently heating to the ageing temperature. This kind of quench sensitivity is thought to be the reason for the poor ageing response of these alloys. The paucity of quenched-in vacancies due to the sinks available at the

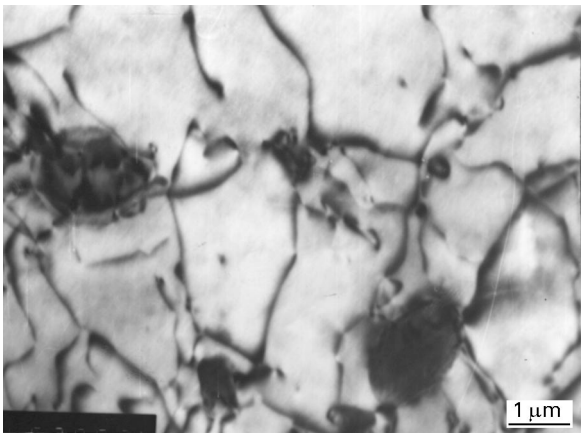

Figure 15 Transmission electron micrograph of alloy 2 in the quenched condition.

insolubles/matrix interface makes the diffusion of chromium sluggish. So collection of a requisite number of chromium atoms for nucleation is delayed and hence an incubation period in the ageing curves is noted.

The beneficial effect of silicon in eliminating the incubation period appears to be due to the reduction in interfacial energy at the precipitate–matrix interface. Silicon is segregated at the dislocation substructure and also in dislocation loops. This helps to nucleate particles of smaller critical nucleus size. Hence the incubation period is lessened. On the contrary, silicon, due to its higher valency, has a higher binding energy with the vacancies though chromium preferentially binds the vacancies. Thus it traps the quenched-in vacancies and delays diffusion of chromium.

The atomic radius of silicon is considerably lower than that of aluminium. Because the atomic radius of chromium is intermediate between them, the replacement of the Al–Si bond by the Al–Cr bond will bring about a local reduction in energy. Thus it may be surmised that the activity of silicon is increased due to chromium. So, under conditions of solute rejection, silicon will give way to chromium atoms to be retained more in the solid solution by being segregated at the dislocation. Therefore, more chromium becomes available for subsequent precipitation during ageing. Thus silicon addition not only delays precipitation but also ensures a greater extent of precipitation during ageing. This is the reason why it reduces the quench sensitivity and delays the chromium precipitation as well. The higher ageing hardness in silicon-bearing alloys is likewise attributed to the greater population of finer precipitates.

Estimation of n and k indicates that silicon addition leads to an increase in the nucleation parameter by 20% whereas the growth parameter essentially remains the same. Also, activation energy remains more or less constant. This means that silicon helps to stimulate nucleation, by reducing the interfacial energy, when chromium precipitates at the dislocations where silicon atoms become segregated.

The results of microhardness testing simply indicate that supersaturation within the matrix solid solution leads to phase decomposition due to ageing in the expected manner. When considered as a whole, hardening by the coarse intermetallics predominates due to the considerably large quantity of the intermetallics, and the age-hardening effect is poorly recorded in macrohardness testing.

The near constancy of yield stress in the case of alloys containing higher chromium content, up to a certain ageing temperature, is due to a balance between the nucleation of precipitate and their growth. The yield strength depends on the population of fine precipitates which pins the dislocation. Because some precipitates grow while some new ones are formed simultaneously, the yield stress remains more or less constant until the ageing temperature becomes so high as to enable the nucleation rate to dominate. However, above a certain temperature, characteristic of the alloys, Oswald's ripening becomes responsible for a decrease in yield stress. Yield stress is relatively insensitive up to 400 °C in alloy 1, beyond which it falls off due to particle coarsening. Without silicon, alloy 1 reaches its saturation precipitate density relatively faster. Because steady state is reached earlier, the yield stress remains more or less constant in the initial stage. However, with a slight increase in the silicon content of the alloy (alloy 4), the critical nucleus size is reduced and the cutting mechanism becomes increasingly operative from relatively lower temperature. At these temperatures, the growth of particles is rather small and so the yield stress rises. The balance between nucleation and growth rate achieved within 400–450 °C corresponds to a constancy in the variation of yield stress with ageing temperature. Beyond this temperature, Oswald's ripening becomes prominent and yield stress falls.

The strain-hardening exponents calculated for the alloys show, in general, a fall in value during the time the yield stress increases. This implies that deformation behaviour of these age-hardenable systems is essentially free of precipitate structure and depends on the matrix properties. As observed in Fig. 15, dislocation tangles established by the particles are responsible for work hardening in these alloys. When aged at higher temperatures, although fresh fine precipitates appear which increase the yield strength, they have little effect on the deformation behaviour in the plastic regime. Ageing at high temperature annihilates dislocations and the density decreases. This automatically reduces the flow stress. This is ultimately reflected in the lower values of n.

5. Conclusions

1. Guinier–Preston zones are not formed in these alloys and age hardening occurs due to precipitation of intermetallics at the dislocation tangles and loops.

2. If the chromium content is higher than the primary solid solubility limit, ageing response becomes poor in the binary alloy, principally owing to premature precipitation of intermetallics on the existing insolubles.

3. Silicon increases the nucleation density in this alloy by way of reducing the interfacial energy at the precipitate/matrix interface. It segregates at the dislocation tangles and small Frank loops, and stimulates nucleation of $CrAl_7$ intermetallics on them. As a result of silicon addition, the ageing response is improved at overall higher ageing hardness.

4. The plastic deformation behaviour of the alloy system is primarily dependent on the matrix structure.

Acknowledgement

The author is greatly indebted to the Board of Research in Nuclear Science, Department of Atomic Energy, Government of India, for its support in carrying out this work (through sanction 34/15/89-G).

References

1. M. HANSEN, in "Constitution of Binary Alloys" (1958) p. 81, and related reference.
2. K. NAGAHAMA and I. MIKI, *Trans. Jpn. Inst. Metals* **15** (1974) 185.
3. H. K. HARDY, *ibid.* **84** (1955–56) 429.
4. M. OHTA, *Trans. Jpn Inst. Metals* **6** (1965) 4.
5. P. CZURRATIS, R. KROGEL, H. LOFFLER, J. LENDVAI and I. KOVACS, "Materials Science Forum", Vol. 13/14 (Trans. Tech. Publications, Aedermannsdorf, Switzerland, 1987) p. 273.

Received 9 May 1995
and accepted 14 July 1997